ChemPubSoc Europe

DOI: 10.1002/open.201700013

Open Access ChemistryOPEN Full Papers

Heterobifunctional Dyes: Highly Fluorescent Linkers Based on Cyanine Dyes

Virginia Wycisk,[a] Katharina Achazi,[a] Ole Hirsch,[b] Christian Kuehne,[c] Jens Dernedde,[c] Rainer Haag,[a] and Kai Licha*[a]

Herein, we present a new synthetic route to cyanine-based heterobifunctional dyes and their application as fluorescent linkers between polymers and biomolecules. The synthesized compounds, designed in the visible spectral range, are equipped with two different reactive groups for highly selective conjugation under physiological conditions. By applying indolenine precursors with functionalized benzenes, we achieved water-soluble asymmetric cyanine dyes bearing maleimido and *N*-hydroxysuccinimidyl functionalities in a three-step synthesis. Spectroscopic characterization revealed good molar absorption coefficients and moderate fluorescence quantum yields. Further reaction with polyethylene glycol yielded dye–polymer conjugates that were subsequently coupled to the antibody cetuximab, often applied in cancer therapy. Successful coupling was confirmed by mass shifts detected by gel electrophoresis. Receptor-binding studies and live-cell imaging revealed that labeling did not alter the biological function. In sum, we provided a successful synthetic pathway to rigid heterobifunctional cyanine dyes that are applicable as fluorescent linkers, for example, for connecting antibodies with macromolecules. Our approach contributes to the field of bioconjugation chemistry, such as antibody–drug conjugates by combining diagnostic and therapeutic approaches.

1. Introduction

Cyanine dyes, originally used as photosensitizers,[1] have attracted much interest because of their application in biomedical imaging, including in biomolecule labeling,[2] nucleic acid detection,[3] and cancer imaging.[4] Cyanine dyes have many advantages over other organic fluorophores owing to their versatility and their broad wavelength tunability. Alteration of the polymethine chain that connects the two nitrogen centers allows one to reach practically every wavelength in the visible to near-infrared spectral region.[5] Moreover, they are extensively employed as fluorescent labels owing to their good photostability, high molar absorption coefficients, and moderate fluorescence quantum yields in aqueous solutions.[6] Generally, cyanine dyes are produced by a straightforward and stepwise synthesis involving condensation of two methylene bases (heterocyclic systems) and a polymethine-forming reagent under basic conditions. Structural diversity is achieved by numerous pre- and postsynthetic modifications by varying the polymethine chain, *meso* substituents, substituents on the nitrogen atom, and heterocyclic substitutions.[2,7]

Within the last decade, numerous attempts have been made to prepare cyanine dyes with improved optical properties; however, to our knowledge, there is only a limited amount of publications reporting the incorporation of two reactive functionalities to generate a heterobifunctional dye. In 2006, Chipon and co-workers published the synthesis of cyanine-based amino acids for application as heterobifunctional linkers in DNA sequencing or solid-phase-synthesis techniques.[8] The pentamethine dyes employed amino and carboxyl groups at the terminal positions of the nitrogen substituents, which allowed subsequent incorporation in a selective solid-phase peptide synthesis. Moreover, a near-IR cyanine dye linker was modified for use as an improved cancer diagnostic imaging agent and in therapy monitoring.[9] The heptamethine dye was equipped with a cell-penetrating peptide at the *meso* position and cytotoxic agents at the end of the N substituents. The connection of a fluorescent dye as a heterobifunctional linker between a targeting protein or polypeptide and a therapeutic agent allows simultaneous targeted imaging and cancer therapy.

Today, the vast majority of bifunctional linkers are based on polyethylene glycol (PEG), which is one of the most widely used biocompatible polymers. PEG is generally used for cova-

[a] *V. Wycisk, Dr. K. Achazi, Prof. Dr. R. Haag, Dr. K. Licha*
Institute of Chemistry and Biochemistry, Freie Universität Berlin
Takustr. 3, 14195 Berlin (Germany)
E-mail: kai.licha@fu-berlin.de

[b] *Dr. O. Hirsch*
Physikalisch-Technische Bundesanstalt
Abbestr. 2–12, 10587 Berlin (Germany)

[c] *C. Kuehne, Dr. J. Dernedde*
Institute of Laboratory Medicine
Clinical Chemistry and Pathobiochemistry
Charité-Universitätsmedizin Berlin
Augustenburger Platz 1, 13353 Berlin (Germany)

Supporting Information for this article can be found under: https://doi.org/10.1002/open.201700013.

lent attachment to macromolecules, proteins, drugs, and vesicles because of its outstanding properties, which include low toxicity, good water solubility, and high flexibility.[10] Upon PEGylation of biomolecules, enhanced solubility and stability as well as reduced clearance from the body and low immunogenicity are observed.[11] The attachment of PEG to serum albumin has been shown to lead to protection from proteolytic degradation and, as a result, elongation of its half-life time.[12] Over the last few years, researchers have concentrated on antibodies and antibody fragments for potential use as therapeutic agents. PEGylation is a well-established method, because the local residence time of antibody fragments can be increased.[11,13] Heterobifunctional linkers are also broadly applied in antibody–drug conjugates. Even though the drug can be directly attached to the biomolecules, the addition of a linker enhances stability and facilitates drug release at the target site.[14] Furthermore, immobilization of antibodies is mainly achieved by heterobifunctional linkers[15] for the analysis, separation, synthesis, and detection of biomolecules.[16] Antibodies are often applied in cancer therapy, but for diagnostic approaches, a fluorescent label must be attached for monitoring biodistribution, which is mainly achieved after linker conjugation. Subsequent labeling of biomolecules might interfere with the functionality, and there are usually only a limited number of binding sites. A fluorescent linker overcomes these problems and can be used in applications for the simultaneous detection and imaging of drug and targeting molecules. Introduction of a drug through a fluorescent linker can also reveal information on the total amount of active species attached to the biomolecules through spectroscopic analysis. The functionality of the biomolecules is less compromised if the number of chemical transformations is reduced. Therefore, bifunctional and fluorescent linkers might be valuable for analytics and might be simultaneously applied in imaging techniques.

Herein, we present an efficient route for the synthesis of cyanine-dye-based linkers bearing two different reactive functional groups. The dyes are equipped with terminal maleimido and *N*-hydroxysuccinimidyl (NHS) ester functionalities for highly efficient biorthogonal cross-linking reactions. Our approach involved the design of dyes in the visible spectral range, each of them bearing either a sulfonic acid or a defined PEG-10 chain to prevent aggregation and to improve solubility properties (Scheme 1). The heterobifunctional dyes were applied in a representative bioconjugation approach by using an IgG antibody and PEG as a polymer to prove their suitability as bifunctional and fluorescent linkers. By gel electrophoresis, we confirmed the successful coupling of polymer–dye conjugates to the antibody and thereby the increase in the molecular weight as a result of PEGylation. Confocal laser scanning microscopy showed the characteristic cell-membrane binding and cellular uptake, which demonstrated that the approach maintained the functionality of the antibody.

2. Results and Discussion

2.1. Dye Synthesis

We synthesized cyanine dyes bearing two different functional groups (maleimides and NHS esters) for their use as fluorescent linkers and subsequent conjugation under physiological conditions. Furthermore, we provided heterobifunctional dyes in the visible spectral range by using two acroleine derivatives

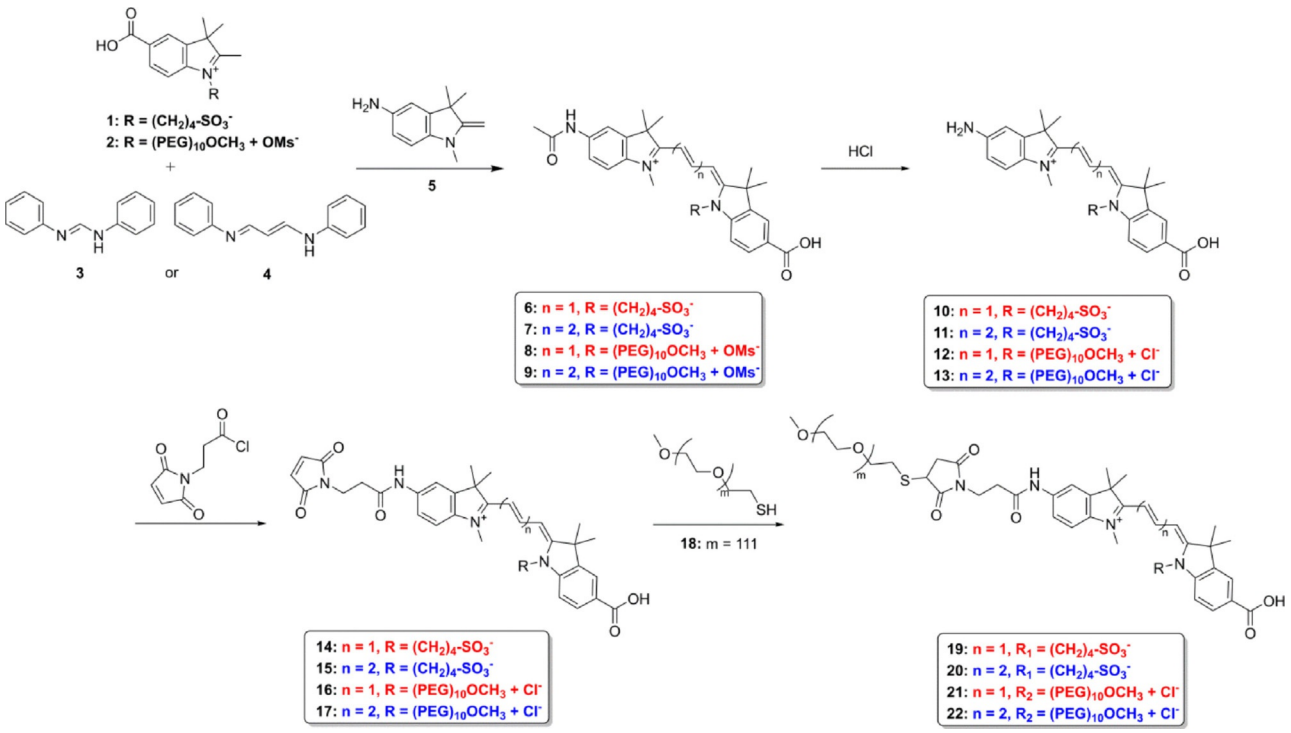

Scheme 1. Synthesis of reactive bifunctional trimethines ($n = 1$) and pentamethines ($n = 2$) with either sulfobutyl or PEG-10 side chains.

commonly used for cyanine dye synthesis. For the synthesis of asymmetric dyes, we started from two different benzene-substituted indolenine precursors that bore either an aromatic amino or a carboxyl group. Moreover, we prepared dyes with different alkylation patterns of the nitrogen atom in the indole moieties. Whereas the amino indolenine precursor was equipped with a methyl group, the carboxylated indolenine carried a polar chain to introduce hydrophilicity and to improve aqueous solubility. Alkyl chains carrying sulfonic acids are generally used to enhance water solubility of a dye and, moreover, to prevent aggregation as a result of electrostatic repulsion. Furthermore, polyether units such as PEGs are known to prevent aggregation by steric shielding. Therefore, we prepared an alkylated indolenine based on a defined mPEG-OH with 11 oxyethylene units that was previously mesylated and treated in a microwave system according to published work to yield 43% of carboxyindolenine **2**.[17] The dye synthesis was performed by heating a mixture of carboxylated indolenine precursor **1** or **2** and *N*,*N*′-diphenylformamide **3** or 3-anilinoacrolein anil **4** in acetic anhydride. In the second step of the reaction, the aminoindolenine and sodium acetate were added, which was followed by the addition of acetic acid; this accelerated dye formation owing to solubilization of the base. In the first part of the synthesis, the aromatic amine was acetylated by acetic anhydride, which generated *N*-acetylated indocarbocyanines (ICCs) **6** and **8** and indodicarbocyanines (IDCCs) **7** and **9** in moderate yields ranging from 21 to 49%. The structures of the ICC and IDCC are based on the well-known Cy3 and Cy5 fluorophores, both of which emit in the visible spectral range. Dyes **6** and **7** carry a sulfobutyl chain, whereas dyes **8** and **9** were alkylated with a PEG-10 chain as described above. The final step to yield the derivatives with free amino and carboxylic acid groups required removal of the acetyl protecting group, which could be accomplished by using aqueous hydrogen chloride and heating in a microwave system to yield dyes **10**–**14** as amino acid derivatives (57–68%). Subsequent reaction of dye **10** with 3-(maleimido)propionic acid *N*-hydroxysuccinimide ester in DMF with increasing temperature did not yield desired amide-functionalized derivative **14**. A possible reason might be the low reactivity of aromatic amino groups towards NHS esters. Therefore, we set our focus on more electrophilic acid chlorides. For further reactions, 3-maleimidopropionic acid was treated with thionyl chloride to yield the corresponding acid chloride. Subsequent coupling to dyes **10**–**13** afforded dyes **14**–**17** in 55–78% yield. After the successful synthesis of the dyes, we tried to achieve the first step in the linking by introducing a polymer moiety (PEG_{5kDa} thiol) to the fluorescent linker. Hence, in the next synthetic step, the maleimide underwent Michael addition with the PEG_{5kDa} thiols, which thereby proved the functionality of the maleimide group. The reaction was conducted in water by using dyes **14**–**17** in excess amounts (2 equiv.) to achieve a nearly quantitative loading. Nonreacted dyes were removed by normal-phase (NP) column chromatography, size-exclusion chromatography, and dialysis. ^{1}H NMR spectroscopy confirmed the absence of unreacted dye and the formation of the Michael–thiol adducts. Indeed, the yield for PEG_{5kDa}ylated dyes **19**–**22** was 31–99%, and a dye loading of nearly one dye per polymer was achieved (see Table 1 for more details). Compound **20** revealed a low loading of 0.5 dyes per polymer, which might be due to solubility issues in aqueous solutions. Dye-labeled PEG_{5kDa} containing PEG-10 chains (compounds **21** and **22**) were prepared in moderate yields (31–39%), most likely as a result of purification by NP column chromatography, on which the compounds either decomposed or interacted with the column material.

2.2. Bioconjugation

To prove suitability as cross-linking fluorescent labels, the newly synthesized dyes were conjugated exemplary to the biomolecule cetuximab (ctx), a monoclonal IgG antibody that targets the epidermal growth factor receptor (EGFR) on tumor cells. Therefore, derivatives with terminal carboxyl functionalities (see compounds **14**–**17** and **19**–**22**) were converted into

Table 1. Spectroscopic data of free dyes **14**–**17** and **19**–**22** and cetuximab conjugates in PBS.[a]

Compd	λ_{abs} [nm]	λ_{em} [nm]	Stokes shift [nm]	ε [$M^{-1}cm^{-1}$]	Φ_f	B[b]	D/P
14	557	580	23	93000	0.028	2604	–
15	655	680	25	127000	0.045	5715	–
16	558	584	26	117000	0.033	3861	–
17	655	678	23	138000	0.062	12696	–
19	560	584	24	–	0.045	–	0.9[c]
20	659	682	23	–	0.061	–	0.5[c]
21	561	586	25	–	0.043	–	0.8[c]
22	658	682	24	–	0.063	–	0.9[c]
ctx–**14**	561	585	24	–	–	–	1.5
ctx–**15**	659	677	18	–	–	–	1.0
ctx–**16**	561	587	26	–	–	–	1.0
ctx–**17**	659	675	16	–	–	–	1.2
ctx–**19**	562	587	25	–	–	–	1.2
ctx–**20**	660	687	27	–	–	–	1.2
ctx–**21**	562	589	27	–	–	–	1.2
ctx–**22**	659	683	24	–	–	–	0.8

[a] λ_{abs}: maximum absorption wavelength, λ_{em}: maximum emission wavelength, ε: molar absorption coefficient, Φ_f: quantum yield, B: brightness, D/P: dye/protein ratio. [b] $B = \varepsilon(\lambda_{abs}) \times \Phi_f$. [c] Dye/polymer ratio.

their respective NHS esters. For sulfobutyl-alkylated dyes (see compounds **14**, **15**, **19**, and **20**) *N*,*N*,*N*′,*N*′-tetramethyl-*O*-(*N*-succinimidyl)uronium hexafluorophosphate (HSTU) was used, whereas dyes with defined PEG-10 chains (see compounds **16**, **17**, **21**, and **22**) were activated with dicyclohexylcarbodiimide (DCC)/*N*-hydroxysuccimide, which showed better results in purification by NP chromatography. Corresponding NHS esters **14a**–**17a** were obtained in good yields ranging from 67 to 97%.

The next step involved labeling of a suited antibody to elucidate the optimal pathway of cross-linking bioconjugation. We applied cetuximab as the antibody owing to our experience in previous work.[17a,18] Cetuximab was treated separately with dyes **14a**–**17a** (2 equiv.), and purification by size-exclusion chromatography revealed bioconjugates ctx–**14** to ctx–**17** with dye/protein ratios (D/P) between 1.0 and 1.5. Subsequent Michael addition with PEG_{5kDa} thiol did not lead to the desired cetuximab conjugates, most likely as a result of the low availability of maleimide functionalities on the antibody. However, the maleimide group functionality was already proven upon conjugating the dyes to the PEG_{5kDa} thiols before bioconjugation (see dye synthesis part). Therefore, we decided to prepare dye-labeled polymers first followed by activation of the carboxylic acids. The corresponding NHS esters were prepared by using the above-described methods in yields of 57 to 91% after purification by size-exclusion or column chromatography. Activated esters of dye-labeled PEG_{5kDa} **19a**–**22a** were conjugated with cetuximab as described above and were additionally purified by affinity chromatography to remove unbound dye-labeled polymers. The absence of free dye was confirmed by gel electrophoresis (see Figure S28 in the Supporting Information).

2.3. Spectroscopic Characterization

Upon comparing solutions of the ICC derivatives bearing amine versus amide functionalities, a color change in the solution from dark purple to pink is visible, whereas dark-blue solutions are observed at every step of the synthesis for the IDCC derivatives. The absorption spectra of amino-functionalized dyes **10**–**13** reveal a broad band with the absence of the characteristic shoulder at $\lambda = 520$ nm for the ICCs and at $\lambda =$ 620 nm for the IDCCs. The effect is even more pronounced for ICC derivatives **10** and **12**. The absorption spectra of IDCC dyes **11** and **13** also reveal a broad band, but the characteristic shoulder is observed. Functionalization of the amine group into an amide group results in narrow bands for all cyanine derivatives, which exhibit spectra with typical bands for the short-wavelength dimer and the main monomer. Figure 1 illustrates the absorption spectra of amine-functionalized dyes **10**–**13** and those of corresponding amide derivatives **14**–**17** bearing the maleimido group. Furthermore, the absorption spectra of dye-labeled PEG_{5kDa} conjugates **19**–**22** are also added to each plot. The absorption spectra reveal a slight increase in the dimer band for the PEG_{5kDa} labeled with sulfodyes, whereas the other derivatives show similar spectra before and after polymer conjugation. Moreover, the absorption spectra in four different solvents [water, phosphate-buffered saline (PBS), DMSO, and methanol] reveal only a slight influence of solvent polarity (Figure S26). The spectra of amido-functionalized dyes **14**–**17** and **19**–**22** show fewer differences in line shape, whereas the absorption spectra of amino dyes **10**–**13** reveal broader bands, particularly for DMSO. Furthermore, all spectra recorded in DMSO show a slight bathochromic shift relative to those recorded in methanol or aqueous solutions. Dyes with sulfobutyl alkylation have spectra similar to those of their respective dyes comprising PEG-10 chains. Table 1 summarizes all of the spectroscopic data obtained for dyes **14**–**17** and **19**–**22** and the cetuximab conjugates. The absorption spectra reveal bathochromically maxima that are shifted by approximately 10 nm for the ICC and IDCC derivatives relative to the spectra of published cyanine dyes with similar constitutions.[2]

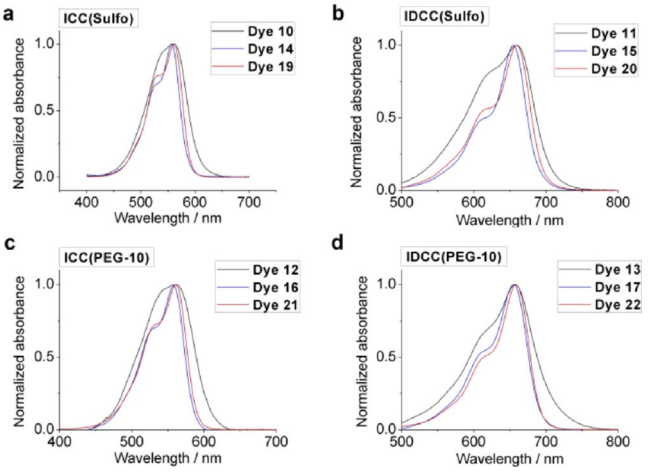

Figure 1. Absorption spectra of dyes **10**–**17** and **19**–**22** in PBS solution.

Furthermore, the new bifunctional dyes exhibit molar absorption coefficients (ε) in the range of 90000 to 140000 $M^{-1}cm^{-1}$, which are lower than those of common cyanine dyes. ICC derivatives **14** and **16** reveal smaller ε values than the IDCC derivatives, whereas dyes alkylated with PEG-10 chains generally exhibit the largest ε values. The newly synthesized cyanine dyes also show moderate quantum yields (Φ_f) between 3 and 6%. The values were determined from the absolute fluorescence quantum yield measurements. For comparison, a sulfo-ICC dye was used, and it revealed a Φ_f value of 4.9%. Trimethine (ICC) dyes are generally known for their low quantum yields, whereas pentamethine (IDCC) dyes exhibit larger Φ_f values.[2,17a,19] However, in 1989 Mujumdar et al. reported the synthesis of cyanine dyes with aromatic amide functionalities and observed similar ε and Φ_f values for the dyes investigated.[20] Comparing dyes alkylated with sulfobutyl and PEG-10, no differences between the ICC derivatives are observed. Comparing dyes conjugated with PEG_{5kDa} with their parent dyes, an increase in Φ_f might be noted, but the difference between them is very small.

2.4. Biological Characterization

Biological evaluation of the newly synthesized labels conjugated to cetuximab and subsequently purified was conducted by

surface plasmon resonance (SPR), gel electrophoresis, and cellular uptake studies by confocal laser scanning microscopy (cLSM). Retained functionality of the dye-labeled antibodies was proven by SPR, and similar affinity constants were revealed for all tested bioconjugates ctx–**14** to ctx–**17** and ctx–**19** to ctx–**22** (see Table S1 and S2). Additionally, gel electrophoresis under reducing conditions, that is sodium dodecyl sulfate polyacrylamide gel electrophoresis (SDS-PAGE), confirmed the absence of free dye and the covalent coupling to the light and heavy chains of cetuximab on a 13% polyacrylamide gel (see Figure S28). Furthermore, separation on a 10% polyacrylamide gel clearly revealed shifted bands of higher molecular weight (+5 kDa) for PEGylated conjugates ctx–**19** to ctx–**22** relative to unlabeled cetuximab and antibodies labeled only with dyes **14**–**17** (see Figure 2). A mass shift of approximately 5 kDa was observed for the heavy and light chains of cetuximab. Those results confirm the functionality of new dyes as suitable bifunctional and fluorescent linkers between polymers and antibodies, here exemplified with a typical IgG antibody and a PEG_{5kDa} polymer. We also recorded images of live cells treated with ctx conjugates by using cLSM for the confirmation of antibody functionality and cellular uptake. EGFR-positive A431 cells were incubated with ctx conjugates for 3 h followed by a washing step. Live-cell images were recorded and revealed characteristic cell-membrane binding for all conjugates tested as well as an accumulation inside cellular compartments (see Figure 3). This is consistent with EGFR expression at the cell surface and internalization upon receptor binding. Considering the amount of dye conjugated (see D/P ratios in Table 1), all conjugates revealed comparable emission intensities. Bioconjugates bearing PEG_{5kDa} showed cell-membrane binding as well as signal accumulation inside the cells. The low EGFR-expressing A549 cell line was used as a control[21] and revealed, as expected, less membrane staining and uptake of antibody conjugates (see Figure S29). We successfully confirmed the functionality of the new dyes as labels for biological application as well as the possibility to combine polymers and antibodies by fluorescent linkers.

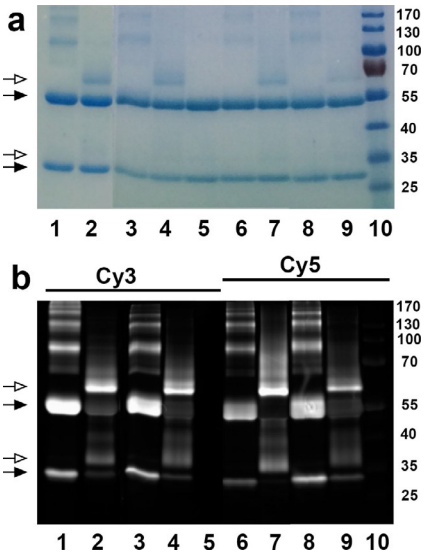

Figure 2. SDS-PAGE of cetuximab conjugates ctx–**14** (lane 1), ctx–**19** (lane 2), ctx–**16** (lane 3), ctx–**21** (lane 4), free ctx (lane 5), ctx–**15** (lane 6) ctx–**20** (lane 7), ctx–**17** (lane 8) ctx–**22** (lane 9), and protein marker (lane 10). The images in panels a and b were obtained under reducing conditions and show the heavy and light antibody chains (black arrows) and respective shifts (white arrows) of Coomassie-stained gel (a) and Cy3/Cy5 fluorescence (b), respectively.

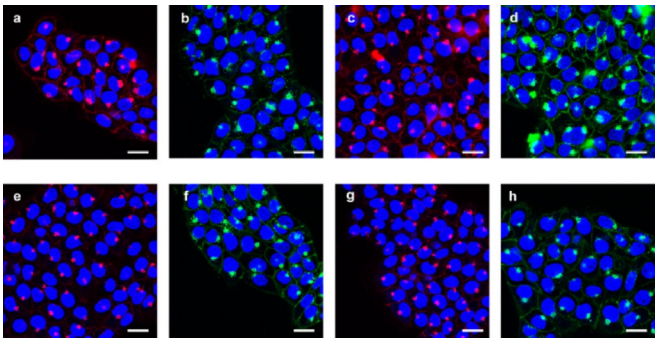

Figure 3. Live-cell images of A431 cells incubated for 3 h with ctx conjugates: a) ctx–**14**, b) ctx–**15**, c) ctx–**16**, and d) ctx–**17**. PEG_{5kDa}ylated conjugates: e) ctx–**19**, f) ctx–**20**, g) ctx–**21**, and h) ctx–**22**. The nucleus was strained with Hoechst (blue). ICC is shown in red and IDCC in green. Scale bars equal 25 μm.

3. Conclusions

We synthesized four bifunctional dyes, each bearing two different functional groups for biorthogonal reactions under physiological conditions. Asymmetric dyes were prepared from benzene-substituted indolenine precursors. Through additional modifications, we were able to introduce reactive maleimido and *N*-hydroxysuccinimidyl (NHS) ester functionalities for chemoselective reactions with thiols and amines, respectively. In summary, four dyes were produced including two different wavelength ranges, Cy3 and Cy5, each of which were designed with different N-alkylation strategies, sulfonic acid and defined polyethylene glycol (PEG)-10 chains. The sulfonic acid moiety increased the hydrophilicity, whereas the defined PEG-10 groups suppressed aggregation and provided flexible solubility in many solvents. Spectroscopic characterization revealed broad absorption bands for amino-substituted dyes. The bands narrowed upon conversion into the amide. Maxima were bathochromically shifted relative to known cyanine dyes, whereas moderate values of the molar absorption coefficients and fluorescence quantum yields up to 140 000 $M^{-1}cm^{-1}$ and 0.06, respectively, were revealed, and these values are comparable to those of other previously reported cyanine dyes.[20] Subsequent Michael addition of PEG_{5kDa} thiols yielded polymer conjugates without inducing aggregation. By successful conversion into NHS esters and bioconjugation with cetuximab, we afforded conjugates with dye/protein ratios between 0.8 and 1.5. Gel electrophoresis confirmed the successful functionalization of the antibodies with dye-labeled PEG_{5kDa} by revealing a mass shift of about 5 kDa, whereas receptor binding studies by surface plasmon resonance proved the biofunctionality of the la-

beled antibodies. Finally, confocal microscopy of living A431 cells demonstrated membrane targeting to epidermal growth factor receptor (EGFR)-positive cells and cellular uptake of cetuximab conjugates. These new heterobifunctional labels, which can be used as fluorescent linkers, yielded bioconjugates on the basis of one single synthetic manipulation of the biomolecules. This strategy is promising for future applications to enable the detection and imaging of more defined conjugates. With respect to a theranostic approach, a targeting moiety can be combined with a second effector molecule (drug) through a fluorescent dye to realize an additional readout.

Experimental Section

Materials and Methods

All solvents and chemicals were commercially purchased from ABCR, Acros Organics, Fluka, Merck, Sigma–Aldrich, ThermoFisher Scientific, or VWR and were used as received unless otherwise stated. *m*-dPEG11-OH was acquired from Quanta BioDesign Ltd., and MeO-PEG_{5kDa}-SH was purchased from Iris Biotech GmbH. HSTU was bought from Carbolution, and indolenine **5** was purchased from Toronto Research. Erbitux was purchased from Merck Serono, and cetuximab was isolated by ultracentrifugation and lyophilization. Synthesized cyanine dyes were purified by preparative HPLC on a high-pressure gradient system (stainless steel) equipped with dual Shimadzu LC-8A pumps, a Shimadzu CBM-20A controller, a variable wavelength UV detector from Knauer, and a Rheodyne injector with a 10 mL sample loop. The stationary phase was a prepacked RP-18 column (RSC-Gel, 5 μm, 20×250 mm) from RSC (Reinhardshagen, Germany). HPLC runs were performed with a total flow rate of 20 mL min^{-1} by applying a gradient from 10 to 100% MeOH with UV detection at $\lambda = 550$ or 650 nm. Purification of lipophilic dyes was done by automated flash chromatography with a Combi Flash R_f+ (Teledyne ISCO) on normal (silica gel, 30 μm) phase. Dialysis was performed with membranes of regenerated cellulose [molecular weight cut-off (MWCO): 1000 or 2000 g mol^{-1}] purchased from Carl Roth. Pure dyes were dried with a Virtis Benchtop K 20K XL, and size-exclusion chromatography was conducted on prepacked Sephadex columns (NAP-25, Sephadex G-25 DNA) or on a glass column (30×2.5 cm) filled with Sephadex G-50 superfine (Sigma–Aldrich) using PBS as solvent. Sensitive substances were shaken in a Bioshake iQ, and centrifugation was conducted with a Universal 32 from Hettich. Reactions in a microwave were performed in a Biotage Initiator+. All sample weights were taken with a Precisa XB120A, and for thin-layer chromatography (TLC), silica gel 60 RP-18 $F_{254}S$ plates were used for reverse-phase analysis and silica gel 60 F_{254} for normal-phase analysis. ^{1}H NMR and ^{13}C NMR spectra were measured with a JEOL ECX, a Bruker AVANCE III 500, or a Bruker AVANCE III 700 spectrometer. Mass spectra were obtained by electrospray with an Agilent 6210 ESI-TOF spectrometer or by matrix-assisted laser desorption ionization time-of-flight mass spectrometry (MALDI-TOF MS) with a Bruker Ultrafex II.

Absorption and Fluorescence Measurements

Samples for absorption and fluorescence measurements were dissolved in Millipore water or PBS solution (3 mm KCl, 140 mm NaCl, 0.01 M $Na_2HPO_4 \cdot 7H_2O$ in 500 mL distilled water). All absorption spectra were acquired with a PerkinElmer LAMBDA 950 UV/VIS/NIR spectrometer by using disposable cuvettes from Brand, and fluorescence spectra were recorded with a Fluorolog 3 fluorometer (Horiba Jobin Yvon). Absolute fluorescence quantum yields were calculated from previously recorded fluorescence spectra with an integrating sphere (80 mm diameter, handmade). Slit widths were set to 2 nm (excitation) and 0.7 nm (emission). ICC dyes were excited at $\lambda = 540$ nm, whereas IDCCs were excited at $\lambda = 640$ nm and the integration time was set to 4 s. For the determination of Φ_f, integrated fluorescence of the sample and solvent were determined to achieve the number of emitted (546–750 nm for ICC and 646–790 nm for IDCC, step size: 2 nm) and absorbed (536–545 nm for ICC and 636–645 nm for IDCC, step size: 0.2 nm) photons. The light intensity was reduced by a neutral density filter (10% transmission) for the determination of absorbed photons. The amount of dyes conjugated to polymers was estimated from the dye's absorption maximum in a 5 μM conjugate solution by using the molar absorption coefficient of the corresponding free dye.[22]

Synthesis of Indolenine Precursors

Indolenine **2**: A mixture of 2,3,3-trimethyl-3*H*-indole-5-carboxylic acid (0.526 g, 2.587 mmol) and previously mesylated *m*-dPEG11-OH[17b] (2 g, 3.363 mmol) in acetonitrile (4 mL) was added to a 2–5 mL reaction vial, and the mixture was heated in a microwave system to 160 °C for 2 h. The solvent was removed under vacuum, and the residue was purified by automated column chromatography (CH_2Cl_2/methanol), which afforded compound **2** (0.896 g, 43%) as a brown oil. Yield: . ^{1}H NMR (400 MHz, [D_4]methanol): $\delta = 8.40$ (s, 1H), 8.31 (d, $J = 8.5$ Hz, 1H), 8.02 (d, $J = 8.5$ Hz, 1H), 4.82 (t, $J = 4$ Hz, 2H), 4.02 (t, $J = 4.9$ Hz, 2H), 3.70–3.40 (m, 43H), 2.69 (s, 3H), 1.67 ppm (s, 6H); HRMS: *m/z*: calcd for $C_{35}H_{60}NO_{13}^+$: 702.4059; found: 702.4144.

Synthesis of Dye Labels

Acetylated dye **6**: 4-(5-Carboxy-2,3,3-trimethyl-3*H*-indol-1-ium-1-yl)-butane-1-sulfonate (**1**; 346 mg, 1.019 mmol) and *N*,*N*′-diphenylformamide **3** (200 mg, 1.019 mmol) were dissolved in acetic anhydride (16 mL), and the mixture was heated to 100 °C for 30 min. A mixture of 1,3,3-trimethyl-2-methyleneindolin-5-amine (192 mg, 1.019 mmol) and sodium acetate (251 mg, 3.057 mmol) dissolved in acetic anhydride (8 mL) was added to the solution, which was followed by the addition of acetic acid (728 μL). The solution was stirred at 100 °C for 1 h before the solvent was removed under vacuum and the residue was precipitated in diethyl ether. The residue was purified by RP-HPLC (water/methanol), and dye **6** (260 mg, 44%) was obtained as a red solid. ^{1}H NMR (400 MHz, [D_4]methanol): $\delta = 8.51$ (t, $J = 13.5$ Hz, 1H), 8.10–8.03 (m, 2H), 7.84 (d, $J = 2.0$ Hz, 1H), 7.56 (dd, $J = 8.6$, 2.0 Hz, 1H), 7.32 (d, $J = 8.7$ Hz, 2H), 6.48 (d, $J = 13.4$ Hz, 2H), 4.16 (t, $J = 8$ Hz, 2H), 3.69 (s, 3H), 2.93 (t, $J = 6.4$ Hz, 2H), 2.15 (s, 3H), 2.07–1.93 (m, 4H), 1.77 (s, 6H), 1.76 ppm (s, 6H); HRMS: *m/z*: calcd for $C_{31}H_{37}N_3NaO_6S^+$: 602.2303; found: 602.2295.

Acetylated dye **7**: According to the procedure outlined for dye **6**, 4-(5-carboxy-2,3,3-trimethyl-3*H*-indol-1-ium-1-yl)butane-1-sulfonate (**1**; 90 mg, 0.266 mmol) was treated with aniline acroleine anil **4** (59 mg, 0.266 mmol) to afford dye **7** as a blue solid (78 mg, 49%). ^{1}H NMR (500 MHz, [D_4]methanol): $\delta = 8.22$ (q, $J = 13.5$ Hz, 2H), 8.08–7.99 (m, 2H), 7.81 (d, $J = 2.1$ Hz, 1H), 7.54 (dd, $J = 8.6$, 2.1 Hz, 1H), 7.27 (dd, $J = 14.6$, 8.4 Hz, 2H), 6.65 (t, $J = 12.4$ Hz, 1H), 6.31 (dd, $J = 13.7$, 5.1 Hz, 2H), 4.11 (t, $J = 6.1$ Hz, 2H), 3.64 (s, 3H), 2.91 (t, $J = 4.6$ Hz, 2H), 2.15 (s, 3H), 1.99–1.94 (m, $J = 3.4$ Hz, 4H), 1.73 ppm (s,

13H); HRMS: *m/z*: calcd for $C_{33}H_{39}N_3NaO_6S^+$: 628.2452; found: 628.2683.

Acetylated dye **8**: Indolenine **2** (0.376 mmol) and *N,N'*-diphenylformamide **3** (0.376 mmol) were dissolved in acetic anhydride (6.7 mL), and the mixture was heated to 100 °C for 30 min. A mixture of 1,3,3-trimethyl-2-methyleneindolin-5-amine (0.376 mmol) and sodium acetate (1.128 mmol) dissolved in acetic anhydride (3.3 mL) was added to the solution, which was followed by the addition of acetic acid (310 μL). The solution was stirred at 100 °C for 1 h before the solvent was removed under vacuum. The residue was purified by automated column chromatography (CH_2Cl_2/methanol) to afford dye **8** as a red solid (29.8 mg, 21%); ^{1}H NMR (500 MHz, [D$_4$]methanol): δ = 8.56 (t, *J* = 13.4 Hz, 1H), 8.20–8.07 (m, 2H), 7.96 (d, *J* = 2.1 Hz, 1H), 7.57 (dd, *J* = 8.6, 2.1 Hz, 1H), 7.43 (d, *J* = 8.4 Hz, 2H), 6.54 (t, *J* = 14.1 Hz, 2H), 4.38 (t, *J* = 5.3 Hz, 2H), 3.94 (t, *J* = 5.1 Hz, 2H), 3.77 (s, 3H), 3.66–3.53 (s, 40H), 3.51 (s, 3H), 2.72 (s, 3H), 2.19 (s, 3H), 1.82 (s, 6H), 1.80 ppm (s, 6H); HRMS: *m/z*: calcd for $C_{50}H_{76}N_3O_{14}^+$: 942.5322; found: 942.5529.

Acetylated dye **9**: According to the procedure outlined for dye **8**, indolenine **2** (0.376 mmol) was treated with aniline acroleine anil **4** (0.376 mmol) to afford dye **9** as a blue solid (113 mg, 31%). ^{1}H NMR (500 MHz, [D$_4$]methanol): δ = 8.29 (t, *J* = 14.2, 1H), 8.19 (t, *J* = 13.1 Hz, 1H), 8.08–8.00 (m, 2H), 7.91 (d, *J* = 2.0 Hz, 1H), 7.55 (dd, *J* = 8.5, 2.0 Hz, 1H), 7.39 (d, *J* = 8.6 Hz, 1H), 7.29 (d, *J* = 8.4 Hz, 1H), 6.65 (t, *J* = 12.5 Hz, 1H), 6.47 (d, *J* = 14.2 Hz, 1H), 6.28 (d, *J* = 13.2 Hz, 1H), 4.26 (t, *J* = 5.3 Hz, 2H), 3.87 (t, *J* = 5.2 Hz, 3H), 3.73 (s, 3H), 3.68–3.52 (m, 40H), 3.51 (s, 3H), 2.70 (s, 9H), 2.16 (s, 3H), 1.82–1.70 ppm (m, 12H). HRMS: *m/z*: calcd for $C_{52}H_{78}N_3O_{14}^+$: 968.5478; found: 968.5472.

Amino acid derivative **10**: Dye **6** (103.5 mg, 0.179 mmol) was dissolved in 2 N HCl (20 mL, 40 mmol) and heated to reflux for 2 h. The solvent was removed under vacuum, and toluene was added to coevaporate HCl. The residue was purified by RP-HPLC (water/methanol) to afford dye **10** (61.5 mg, 64%) as a dark-purple solid. ^{1}H NMR (400 MHz, [D$_4$]methanol): δ = 8.49 (t, *J* = 13.6 Hz, 1H), 8.16–8.10 (m, 3H), 7.39 (t, *J* = 8.1 Hz, 2H), 7.22 (d, *J* = 2.0 Hz, 1H), 7.13 (dd, *J* = 8.3, 2.1 Hz, 1H), 6.57 (d, *J* = 10.8 Hz, 1H), 6.49 (d, *J* = 13.1 Hz, 1H), 4.16 (t, *J* = 8 Hz, 2H), 3.73 (s, 3H), 2.92 (t, *J* = 6.8 Hz, 2H), 2.01–1.91 (m, 4H), 1.78 (s, 6H), 1.77 ppm (s, 7H); HRMS: *m/z*: calcd for $C_{29}H_{35}N_3NaO_5S^+$: 560.2190; found: 560.2189.

Amino acid derivative **11**: A solution of dye **7** (50 mg, 0.083 mmol) in acetonitrile (2 mL) and 2 N HCl (2 mL, 4 mmol) was added to a 2–5 mL reaction vial, and the mixture was heated in a microwave system to 100 °C for 2 h. The solvent was removed under vacuum, and toluene was added to coevaporate HCl. The residue was purified by RP-HPLC (water/methanol), and dye **11** (31.7 mg, 68%) was afforded as a blue solid. ^{1}H NMR (400 MHz, [D$_4$]methanol): δ = 8.12 (dd, *J* = 14.3, 11.9 Hz, 1H), 8.03–7.93 (m, 3H), 7.17 (d, *J* = 8.5 Hz, 1H), 7.10 (d, *J* = 8.2 Hz, 1H), 6.84 (d, *J* = 2.2 Hz, 1H), 6.73 (dd, *J* = 8.5, 2.2 Hz, 1H), 6.57 (t, *J* = 12.4 Hz, 1H), 6.39 (d, *J* = 14.3 Hz, 1H), 6.09 (d, *J* = 13.1 Hz, 1H), 3.98 (t, *J* = 7.4 Hz, 2H), 3.68 (s, 3H), 2.89 (t, *J* = 6.0 Hz, 2H), 1.99–1.87 (m, 4H), 1.69 ppm (s, 12H); HRMS: *m/z*: calcd for $C_{31}H_{38}N_3O_5S^+$: 564.2527; found: 564.2512.

Amino acid derivative **12**: A solution of dye **8** (73.7 mg, 0.078 mmol) in acetonitrile (2.5 mL) and 2 N HCl (2.5 mL, 5 mmol) was poured into a 2–5 mL reaction vial, and the mixture was heated in a microwave system to 100 °C for 2 h. The solvent was removed under vacuum, and toluene was added to coevaporate HCl. The residue was purified by automated column chromatography (CH_2Cl_2/methanol) to yield dye **12** (45.7 mg, 65%) as a dark-purple solid. ^{1}H NMR (500 MHz, [D$_4$]methanol): δ = 8.41 (t, *J* = 13.5 Hz, 1H), 8.08–8.01 (m, 2H), 7.32 (d, *J* = 8.7 Hz, 1H), 7.24 (d, *J* = 8.6 Hz, 1H), 6.89 (d, *J* = 2.2 Hz, 1H), 6.78 (dd, *J* = 8.5, 2.2 Hz, 1H), 6.52 (d, *J* = 14.0 Hz, 1H), 6.37 (d, *J* = 12.8 Hz, 1H), 4.28 (t, *J* = 5.2 Hz, 2H), 3.90 (t, *J* = 5.1 Hz, 2H), 3.75 (s, 3H), 3.67–3.52 (m, 40H), 3.51 (s, 3H), 2.73 (s, 2H), 1.78 (s, 6H), 175 ppm (s, 6H); HRMS: *m/z*: calcd for $C_{48}H_{74}N_3O_{13}^+$: 900.5216; found: 900.5246.

Amino acid derivative **13**: According to the procedure outlined for amino acid derivative **12**, dye **9** (113 mg) afforded dye **13** (61.6 mg, 57%) as a blue solid. ^{1}H NMR (500 MHz, [D$_4$]methanol): δ = 8.14 (dd, *J* = 14.6, 11.7 Hz, 1H), 8.07–7.92 (m, 3H), 7.25 (d, *J* = 8.5 Hz, 1H), 7.16 (d, *J* = 8.3 Hz, 1H), 6.86 (d, *J* = 2.2 Hz, 1H), 6.76 (dd, *J* = 8.5, 2.2 Hz, 1H), 6.58 (t, *J* = 12.5 Hz, 1H), 6.51 (d, *J* = 14.5 Hz, 1H), 6.11 (d, *J* = 12.9 Hz, 1H), 4.16 (t, *J* = 5.3 Hz, 2H), 3.84 (t, *J* = 5.3 Hz, 2H), 3.75 (s, 3H), 3.65–3.53 (m, 40H), 3.52 (s, 3H), 2.71 (s, 1H), 1.71 ppm (s, 12H); HRMS: *m/z*: calcd for $C_{50}H_{76}N_3O_{13}^+$: 926.5373; found: 926.5363.

Maleimide derivative **14**: A mixture of dye **10** (33.3 mg, 0.123 mmol), 3-maleimidopropionic acid chloride (105 mg, 0.560 mmol), and iPr_2NEt (32 μL, 0.186 mmol) in DMF (3 mL) was stirred at 50 °C for 1 h. The mixture was precipitated in diethyl ether, and the residue was purified by RP-HPLC (water/methanol) to afford dye **14** (32.3 mg, 75%) as a red solid. ^{1}H NMR (400 MHz, [D$_4$]methanol): δ = 8.52 (t, *J* = 13.5 Hz, 1H), 8.11 (dd, *J* = 6.5, 1.8 Hz, 2H), 7.88 (d, *J* = 2.0 Hz, 1H), 7.50 (dd, *J* = 8.7, 2.0 Hz, 1H), 7.38 (t, *J* = 8.2 Hz, 2H), 6.83 (s, 2H), 6.57 (d, *J* = 13.9 Hz, 1H), 6.49 (d, *J* = 12.9 Hz, 1H), 4.15 (t, *J* = 7.1 Hz, 2H), 3.89 (t, *J* = 6.9 Hz, 2H), 3.74 (s, 3H), 2.91 (t, *J* = 6.7 Hz, 2H), 2.74–2.64 (t, *J* = 8 Hz, 2H), 2.06–1.91 (m, 5H), 1.78 (s, 6H), 1.76 ppm (s, 6H); ^{13}C NMR (176 MHz, [D$_4$]methanol): δ = 177.56, 174.96, 172.20, 171.38, 169.25, 151.88, 147.39, 143.24, 141.92, 139.94, 138.67, 135.53, 132.47, 128.54, 124.65, 121.65, 115.71, 113.18, 111.58, 106.03, 103.90, 51.60, 51.20, 49.52, 44.89, 36.56, 35.26, 32.28, 28.46, 27.98, 26.92, 23.47 ppm; HRMS: *m/z*: calcd for $C_{36}H_{40}N_4NaO_8S^+$: 711.2459; found: 711.2487.

Maleimide derivative **15**: A mixture of dye **11** (45.4 mg, 0.08 mmol), 3-maleimidopropionic acid chloride (75.5 mg, 0.402 mmol), and iPr_2NEt (41.4 μL, 0.240 mmol) was dissolved in dimethylacetamide (3 mL), and the mixture was stirred at 50 °C for 3 h. The mixture was precipitated in diethyl ether, and the residue was purified by RP-HPLC (water/methanol) to give dye **15** (31.7 mg, 55%) as a blue solid. ^{1}H NMR (700 MHz, [D$_6$]DMSO): δ = 10.25 (s, 1H), 8.33 (t, *J* = 13.3 Hz, 1H), 8.23 (t, *J* = 12.6 Hz, 1H), 8.06 (s, 1H), 7.93 (s, 1H), 7.91 (d, *J* = 3.5 Hz, 1H), 7.48 (d, *J* = 9.1 Hz, 1H), 7.44 (d, *J* = 8.4 Hz, 1H), 7.34 (d, *J* = 8.3 Hz, 1H), 7.03 (s, 2H), 6.57 (t, *J* = 11.9 Hz,1H), 6.43 (d, *J* = 14 Hz, 1H), 6.24 (d, *J* = 13.3 Hz, 1H), 4.02 (s, 2H), 3.71 (t, *J* = 7 Hz, 2H), 3.68 (s, 3H), 2.61 (t, *J* = 7 Hz, 2H), 1.76–1.72 (m, 4H), 1.67 (s, 6H), 1.66 ppm (s, 6H); ^{13}C NMR (176 MHz, [D$_6$]DMSO): δ = 174.87, 170.78, 169.71, 168.58, 167.02, 154.53, 152.10, 146.23, 142.15, 140.57, 137.91, 137.44, 134.62, 130.53, 126.20, 125.41, 123.21, 119.31, 113.52, 112.36, 109.72, 105.90, 102.39, 50.67, 49.63, 47.70, 42.97, 34.99, 33.79, 31.81, 27.31, 26.73, 25.65, 22.46 ppm; HRMS: *m/z*: calcd for $C_{38}H_{42}N_4NaO_8S^+$: 737.2616; found: 737.2647.

Maleimide derivative **16**: A mixture of dye **12** (41.2 mg, 0.046 mmol), 3-maleimidopropionic acid chloride (43.1 mg, 0.230 mmol), and iPr_2NEt (23.4 μL, 0.138 mmol) was dissolved in DMF (1.6 mL), and the mixture was stirred at 50 °C for 2 h. The solvent was removed under vacuum, and the residue was purified by automated column chromatography (CH_2Cl_2/methanol) to give dye **16** (27.8 mg, 57%). ^{1}H NMR (700 MHz, [D$_4$]methanol): δ = 8.54 (t, *J* = 13.4 Hz, 1H), 8.13–8.07 (m, 2H), 7.90 (d, *J* = 2.1 Hz, 1H), 7.52 (dd, *J* = 8.6, 2.0 Hz, 1H), 7.41 (m, 2H), 6.84 (s, 2H), 6.55 (d, *J* = 13.8 Hz, 1H), 6.52 (d, *J* = 13.2 Hz, 1H), 4.36 (t, *J* = 5.1 Hz, 2H), 3.92

(t, J = 5.0 Hz, 2H), 3.89 (t, J = 6.9 Hz, 2H), 3.75 (s, 3H), 3.64–3.47 (m, 45H), 2.70 (t, J = 7.0 Hz, 2H), 1.80 (s, 6H), 1.78 ppm (s, 6H); ^{13}C NMR (176 MHz, [D$_4$]methanol): δ = 177.57, 175.60, 172.20, 171.38, 169.10, 151.76, 148.05, 143.23, 141.73, 139.86, 138.79, 135.54, 132.20, 128.16, 124.53, 121.65, 115.68, 113.32, 112.34, 105.96, 104.35, 72.94, 72.08, 71.51, 69.07, 51.23, 49.88, 45.69, 36.53, 35.23, 32.43, 28.56, 27.98 ppm; HRMS: m/z: calcd for $C_{55}H_{79}N_4O_{16}^+$: 1051.5486; found: 1051.5565.

Maleimide derivative **17**: A mixture of dye **13** (51.4 mg, 0.055 mmol), 3-maleimidopropionic acid chloride (31 mg, 0.165 mmol), and iPr_2NEt (28 µL, 0.165 mmol) was dissolved in CH_2Cl_2 (4 mL), and the mixture was stirred at RT for 2 h. The solvent was removed under vacuum, and the residue was purified by automated column chromatography (CH_2Cl_2/methanol) to give dye **17** (46.1 mg, 78%) as a blue solid. ^{1}H NMR (700 MHz, [D$_4$]methanol): δ = 8.27 (t, J = 13.3 Hz, 1H), 8.20 (t, J = 13.0 Hz, 1H), 8.04–8.03 (d, J = 9.1 Hz, 1H), 8.02 (s, 1H), 7.84 (d, J = 2.1 Hz, 1H), 7.51 (dd, J = 8.5, 2.1 Hz, 1H), 7.35 (d, J = 9.1 Hz, 1H), 7.27 (d, J = 8.3 Hz, 1H), 6.84 (s, 2H), 6.65 (t, J = 12.4 Hz, 1H), 6.43 (d, J = 13.0, 1H), 6.30 (d, J = 13.4 Hz, 1H), 4.27 (t, J = 5.3 Hz, 2H), 3.90–3.87 (m, 4H), 3.71 (s, 3H), 3.65–3.52 (m, 40H), 3.51 (s, 3H), 2.69 (t, J = 6.9 Hz, 2H), 1.74 (s, 6H), 1.73 ppm (s, 6H); ^{13}C NMR (176 MHz, [D$_4$]methanol): δ = 176.87, 173.13, 172.23, 171.38, 171.18, 156.00, 153.84, 147.60, 143.74, 141.78, 140.02, 138.45, 135.54, 131.81, 129.86, 127.51, 124.29, 121.53, 115.68, 112.99, 111.29, 106.67, 104.45, 72.88, 72.13, 71.39, 69.14, 59.11, 51.27, 49.56, 45.25, 36.56, 35.26, 32.23, 28.24, 27.59 ppm; HRMS: m/z: calcd for $C_{57}H_{81}N_4O_{16}^+$: 1077.5642; found: 1077.5646.

PEG$_{5kDa}$ conjugate **19**: MeO-PEG$_{5kDa}$-SH **18** (20 mg, 4.0 µmol) and dye **14** (5.6 mg, 8.0 µmol) were dissolved in water (500 µL), and the mixture was stirred at RT overnight. The solvent was removed under vacuum, and the crude product was purified by Sephadex columns (G-50, eluent: water) and dialysis (MWCO: 1000 g mol^{-1}, solvent: water) to give dye **19** (20 mg, 91%) as a red solid. ^{1}H NMR (700 MHz, [D$_4$]methanol): δ = 8.55 (t, J = 13.4 Hz, 1H), 8.12 (s, 2H), 7.92 (s, 1H), 7.58 (d, J = 8.4 Hz, 1H), 7.40 (dd, J = 8.5, 4.3 Hz, 2H), 6.59 (d, J = 13.6 Hz, 1H), 6.53 (d, J = 13.1 Hz, 1H), 4.20 (t, J = 7.4 Hz, 2H), 4.10 (dd, J = 9.0, 3.9 Hz, 1H), 3.96–3.88 (4H), 3.81–3.50 (s, dye: N-CH$_3$, PEG: OCH$_2$, O-CH$_3$), 3.27 (dd, J = 18.7, 9.2 Hz, 2H), 3.08 (dt, J = 12.7, 5.9 Hz, 1H), 2.95 (t, J = 6.8 Hz, 2H), 2.83 (dt, J = 13.2, 6.1 Hz, 1H), 2.74 (t, J = 7.1 Hz, 2H), 2.60 (dd, J = 18.5, 3.9 Hz, 1H), 2.12–1.94 (m, 4H), 1.82 (s, 6H), 1.81 ppm (s, 6H); MS (MALDI-TOF): m/z: 5668.668.

PEG$_{5kDa}$ conjugate **20**: According to the procedure outlined for PEG$_{5kDa}$ conjugate **19**, dye **15** gave dye **20** (23 mg, 99%) as a blue solid. ^{1}H NMR (700 MHz, [D$_4$]methanol): δ = 8.22 (q, J = 13.3 Hz, 1H), 8.08–7.97 (m, 1H), 7.83 (s, 1H), 7.55–7.51 (m, 1H), 7.29 (d, J = 8.5 Hz, 1H), 7.26 (d, J = 8.2 Hz, 1H), 6.67 (t, J = 12.4 Hz, 0H), 6.37–6.26 (m, 2H), 4.12 (s, 2H), 3.95–3.45 (m, dye: N-CH$_3$, PEG: OCH$_2$, O-CH$_3$), 3.26–3.18 (m, 2H), 3.05 (dt, J = 12.7, 6.0 Hz, 1H), 2.95–2.87 (m, 2H), 2.79 (dt, J = 14.1, 6.1 Hz, 1H), 2.70 (t, J = 7.3 Hz, 2H), 2.61–2.52 (m, 1H), 1.98 (m, J = 3.6 Hz, 4H), 1.73 ppm (s, 12H).); MS (MALDI-TOF): m/z: 5737.27.

PEG$_{5kDa}$ conjugate **21**: MeO-PEG$_{5kDa}$-SH **18** (19 mg, 3.8 µmol) and dye **16** (8 mg, 7.6 µmol) were dissolved in water (500 µL), and the mixture was stirred at RT overnight. The solvent was removed under vacuum, and the crude product was purified by automated column chromatography (CH_2Cl_2/methanol) and dialysis (MWCO: 2000 g mol^{-1}, solvent: water). Lyophilization yielded dye **21** (9 mg, 39%) as a red solid. ^{1}H NMR (700 MHz, [D$_4$]methanol): δ = 8.54 (t, J = 13.4 Hz, 1H), 8.10–8.05 (m, 1H), 8.06–8.02 (m, 1H), 7.87 (d, J = 2.0 Hz, 1H), 7.60–7.53 (m, 1H), 7.36 (d, J = 8.6 Hz, 1H), 7.34 (d, J = 8.4 Hz, 1H), 6.51 (d, J = 13.4 Hz, 1H), 6.46 (d, J = 13.7 Hz, 1H), 4.37 (t, J = 5.2 Hz, 2H), 4.08–3.97 (m, 1H) 3.93 (t, J = 5.3 Hz, 2H), 3.91–3.53 (m, dye: N-CH$_3$, PEG: OCH$_2$, O-CH$_3$), 3.15–3.12 (m, 1H), 3.09–3.03 (m, 2H), 2.84–2.77 (m, 1H), 2.71 (t, J = 7.1 Hz, 2H), 2.58–2.55 (m, 1H), 1.79 (s, 6H), 1.78 ppm (s, 6H); MS (MALDI-TOF): m/z: 5815.17.

PEG$_{5kDa}$ conjugate **22**: According to the procedure outlined for PEG$_{5kDa}$ conjugate **21**, dye **17** gave dye **22** (7.4 mg, 31%) as a blue solid. ^{1}H NMR (700 MHz, [D$_4$]methanol): δ = 8.55 (s, 1H), 8.26–8.21 (m, 2H), 8.02 (s, 1H), 8.00 (s, 1H), 7.84 (s, 1H), 7.59–7.48 (m, 1H), 7.31 (d, J = 8.5 Hz, 1H), 7.26 (d, J = 8.2 Hz, 1H), 6.62 (t, J = 12.4 Hz, 1H), 6.35 (dd, J = 13.7, 4.3 Hz, 2H), 4.31 (s, 1H), 4.08–4.06 (m, 1H) 3.93–3.84 (m, 4H), 3.77–3.51 (m, dye: N-CH$_3$, PEG: OCH$_2$, O-CH$_3$), 3.27–3.20 (m, 3H), 3.08–3.04 (m, 1H), 2.85–2.78 (m, 2H), 2.70 (t, J = 7.1 Hz, 3H), 2.57 (dd, J = 16.6, 5.5 Hz, 1H), 1.75 (s, 8H), 1.74 ppm (s, 7H); MS (MALDI-TOF): m/z: 5840.393.

NHS ester **14a**: A mixture of dye **14** (20 mg, 0.029 mmol), HSTU (16 mg, 0.044 mmol), and iPr_2NEt (8 µL, 0.044 mmol) in DMF (555 µL) was stirred at RT overnight. The crude product was precipitated in diethyl ether and centrifuged, and dye **14a** (22 mg, 96%) was obtained as a red solid. ^{1}H NMR (400 MHz, [D$_6$]DMSO): δ = 10.28 (s, 1H), 8.30 (t, J = 13.3 Hz, 1H), 8.23 (d, J = 1.7 Hz, 1H), 8.13 (d, J = 8.5 Hz, 1H), 7.86 (s, 1H), 7.61–7.53 (m, 3H), 7.04 (s, 2H), 6.70 (d, J = 13.8 Hz, 1H), 6.53 (d, J = 13.7 Hz, 1H), 4.08 (s, 2H), 3.75 (s, 3H), 3.73–3.71 (m, 2H), 2.91 (s, 4H), 1.81–1.76 (m, 4H), 1.73 (s, 6H), 1.69 ppm (s, 6H); HRMS: m/z: calcd for $C_{40}H_{43}N_5NaO_{10}S^+$: 808.2631; found: 808.2680.

NHS ester **15a**: According to the procedure outlined for NHS ester **14a**, dye **15** (8.5 mg) gave dye **15a** (10.1 mg, 97%) as a blue solid. ^{1}H NMR (500 MHz, [D$_6$]DMSO): δ = 10.26 (s, 1H), 8.38 (t, J = 14 Hz, 1H), 8.23 (t, J = 13.0 Hz, 1H), 8.19 (s, 1H), 8.06 (dd, J = 8.4, 1.8 Hz, 1H), 7.95 (s, 1H), 7.52 (d, J = 8.6 Hz, 1H), 7.47 (dd, J = 8.7, 1.8 Hz, 1H), 7.42 (d, J = 8.6 Hz, 1H), 7.04 (s, 2H), 6.64 (t, J = 12.4 Hz, 1H), 6.58 (d, J = 14.5 Hz, 1H), 6.26 (d, J = 13.1 Hz, 1H), 4.00 (s, 2H), 3.77–3.69 (m, 5H), 3.73 (s, 2H), 2.91 (s, 4H), 2.64–2.61 (m, 2H), 1.76–1.72 (m, 4H), 1.71 (s, 6H), 1.68 ppm (s, 6H); HRMS: m/z: calcd for $C_{42}H_{45}N_5NaO_{10}S^+$: 834.2779; found: 834.2793.

NHS ester **16a**: A mixture of dye **16** (23.8 mg, 0.023 mmol), N-hydroxysuccimide (7.9 mg, 0.069 mmol), and DCC (14.2 mg, 0.069 mmol) in CH_2Cl_2 (1.5 mL) was stirred at RT overnight. The crude product was purified by automated column chromatography (CH_2Cl_2/methanol) to afford dye **16a** (18.2 mg, 67%) as a red solid. ^{1}H NMR (500 MHz, [D]chloroform): δ = 10.91 (s, 1H), 8.22 (s, 1H), 8.34 (t, J = 13.1, 1H), 8.27 (d, J = 1.9 Hz, 1H), 8.15 (dd, J = 8.5, 1.7 Hz, 1H), 8.01 (d, J = 1.7 Hz, 2H), 7.87 (d, J = 10 Hz, 1H), 7.28 (s, 1H), 7.01 (d, J = 8.6 Hz, 1H), 6.89 (d, J = 13.7 Hz, 1H), 6.73–6.69 (m, 1H), 6.67 (s, 2H), 4.29 (s, 2H), 3.91 (t, J = 7.0 Hz, 2H), 3.94–3.90(m, 5H), 3.64–3.51 (m, 45H), 2.99–2.93 (m, 6H), 1.74 (s, 6H), 1.69 ppm (s, 6H); HRMS: m/z: calcd for $C_{59}H_{82}N_5O_{18}^+$: 1148.5727; found: 1148.5727.

NHS ester **17a**: According to the procedure outlined for NHS ester **16a**, dye **17** (14.7 mg) gave dye **17a** (11.9 mg, 69%) as a blue solid. ^{1}H NMR (500 MHz, [D]chloroform): δ = 11.03 (s, 1H), 8.22 (s, 1H), 8.10 (dd, J = 8.3, 1.8 Hz, 1H), 8.01–7.87 (m, 3H), 7.76 (t, J = 13.0 Hz, 1H), 7.10 (dd, J = 8.8, 3.7 Hz, 2H), 6.67 (s, 2H), 6.65–6.53 (m, 2H), 6.01 (d, J = 12.7 Hz, 1H), 4.09 (s, 2H), 3.91 (t, J = 7.0 Hz, 2H), 3.82 (s, 5H), 3.67–3.49 (m, 45H), 3.00–2.88 (m, 6H), 1.72 (s, 6H), 1.66 ppm (s, 6H); HRMS: m/z: calcd for $C_{61}H_{84}N_5O_{18}^+$: 1174.5806; found: 1174.5945.

NHS ester **19a**: HSTU (0.6 mg, 1.583 μmol) from a stock solution in DMF (6 mg mL^{-1}) and iPr_2NEt (0.5 μL, 1.583 μmol) were added to a solution of dye **19** (6 mg, 1.055 μmol) in DMF (460 μL). The mixture was stirred at RT overnight. The solvent was removed under vacuum, and the crude product was purified by Sephadex columns (NAP-25, Amersham; eluent: water). After lyophilizing, dye **19a** (3.5 mg, 57%) was obtained as a red solid. MS (MALDI-TOF): *m/z*: 5749.21.

NHS ester **20a**: According to the procedure outlined for NHS ester **19a**, dye **20** (10 mg) gave dye **20a** (9.3 mg, 91%) as a blue solid. MS (MALDI-TOF): *m/z*: 5596.130.

NHS ester **21a**: *N*-Hydroxysuccimide (0.52 mg, 4.5 μmol) and DCC (0.93 mg, 4.5 μmol) from stock solutions in DMF (5.6 and 6.4 mg mL^{-1}, respectively) were added to a solution of dye **21** (18 mg, 3 μmol) in DMF (762.5 μL), and the mixture was stirred at RT overnight. The solvent was removed under vacuum, and the residue was purified by automated column chromatography (CH_2Cl_2/methanol) to give dye **21a** (11.4 mg, 62%) as a red solid. MS (MALDI-TOF): *m/z*: 5905.82.

NHS ester **22a**: According to the procedure outlined for NHS ester **21a**, dye **22** (10 mg) gave dye **22a** (6.4 mg, 63%) as a blue solid. MS (MALDI-TOF): *m/z*: 6020.26.

Preparation of Bioconjugates

NHS ester **14a**–**17a** or **19a**–**22a** from a stock solution in PBS (0.4–3.8 mg mL^{-1}) was added to a solution of cetuximab (41 μm) in PBS (pH 7.4) by using a molar excess of the reactive dye (2–8 molecular equivalents). The mixture was gently shaken at RT overnight. Purification of ctx–**14** to ctx–**17** was performed with Sephadex columns and PBS as eluent, whereas conjugates ctx–**19** to ctx–**22** were additionally purified by affinity chromatography by using the following procedure. Reaction solutions of ctx conjugates were passed once over 0.5 mL protein A plus agarose columns (Pierce) equilibrated with PBS (20 mm sodium phosphate, 150 mm NaCl, pH 8.0). The columns were further washed with 5 mL each of PBS, PBS high salt (1 M NaCl), PBS Tween 20 (0.5%), and once again with PBS. Elution of column-bound conjugates was done with 1.6 mL elution buffer (0.1 M glycine, pH 3.0), whereas the eluates were dropped into 0.4 mL of neutralization solution (1 M Tris, pH 9.0). Eluates were further concentrated and desalted on an Amicon Ultra-30K filtration devices (Millipore) by five repeating steps of centrifugation (Megafuge 2R, Thermo Scientific) at 3000×g and refilled to 4 mL PBS. Absence of free dye was confirmed by thin-layer chromatography (RP-C18 TLC) and SDS-PAGE. The D/P ratio of dye–cetuximab conjugates was calculated by using the absorption maximum method.[2,23] Protein concentration of cetuximab was calculated by measuring the absorbance at $\lambda = 280$ nm by using extinction coefficients estimated by the Expasy Protparam tool for ctx.

SPR Binding Studies

Experiments were performed with a Biacore X100 device (GE Healthcare, Freiburg, Germany). A carboxymethylated dextran chip (CM5-Chip, GE Healthcare, Freiburg, Germany) was fully coupled on Fc2 with EGF-R Fc-chimera (R&D Systems, Wiesbaden-Nordenstadt, Germany) by using the amine coupling strategy [1-ethyl-3-(3-dimethylaminopropyl)carbodiimide/*N*-hydroxysuccinimide], HBS-EP [10 mM 4-(2-hydroxyethyl)-1-piperazineethanesulfonic acid (HEPES) pH 7.4, 150 mm NaCl, 3 mm ethylenediaminetetraacetic acid (EDTA) and 0.005% v/v surfactant P20] as a running buffer and acetate pH 4.5 as sample buffer for the ligand. The response level reached for Fc2 was about 4900–5100 RU. Bevacizumab (Avastin, Roche/Genentech) was coupled to Fc1 as a nonbinding control and reached around 15000–22000 RU (see Tables S1 and S2). Affinities were measured by using a kinetic titration series (single cycle kinetics) at 25 °C, in which five ascending concentrations of ctx conjugates were injected consecutively for 120 s at 30 μL min^{-1} followed by a dissociation time of 600 s and two short pulses of 20 s 10 mm glycin HCl pH 2.5 to regenerate the sensor surface. Therefore, conjugates were diluted in running buffer (HBS-EP) at concentrations of 1000, 100, 10, 1, and 0.1 nM. The signal of the Bevacizumab treated flow cell was subtracted from the binding signal. Additionally, blank injects of running buffer were also subtracted (double referencing) for each run. Measurements were done in triplicate. Sensorgrams were analyzed by plotting the analyte concentration against the binding signal at the end of injection. The resulting isotherm was fitted to obtain the equilibrium dissociation constants (K_D) between the antibody and its receptor using the steady-state model.

Cell Studies

For confocal laser scanning microscopy, the epithelial human cancer cell line A431 (DSMZ No. ACC 91) and the human lung carcinoma epithelial cell line A549 (DSMZ No. ACC 107) were routinely propagated in Dulbecco's modified Eagle's medium (DMEM), with 2% glutamine, penicillin/streptomycin (all from Gibco BRL, Eggenstein, Germany), and 10% fetal calf serum (FCS, Biochrom AG, Berlin, Germany) at 37 °C with 5% CO_2 and were subcultured twice a week. For confocal microscopy, 27000 cells were seeded in each well of a μ-Slides 8 Well (ibidi GmbH, Martinsried, Germany) and were cultured at 37 °C for 24 h. Thereafter, dye-labeled test substances were added to the cells at a final concentration of 1 μm. Confocal images were taken with an inverted confocal laser scanning microscope Leica DMI6000CSB SP8 (Leica, Wetzlar, Germany) with a 63×/1.4 HC PL APO CS2 oil immersion objective at 37 °C using the manufacture given LAS X software. Images of different groups were acquired with the same laser and detector settings by using the Leica LAS AF software. The fluorescence detection was performed sequentially for each channel set with the acousto optical beam splitter between $\lambda = 570$ and 648 nm for the ICC dye and between $\lambda = 650$ and 749 nm for IDCC dyes. ICC was excited using the $\lambda = 561$ nm diode-pumped solid-state laser line, whereas IDCC dyes were excited with a $\lambda = 633$ nm HeNe laser.

Acknowledgements

The authors acknowledge the Core Facility BioSupraMol of the Freie Universität Berlin for their technical support and thank the SFB765 as well as the Helmholtz Association for funding of this work through Helmholtz-Portfolio Topic "Technology and Medicine".

Conflict of Interest

The authors declare no conflict of interest.

Keywords: antibodies · conjugation · dyes/pigments · fluorescence · heterobifunctional linkers

[1] R. M. Christie, *Colour Chemistry* (Ed.: R. M. Christie), Royal Society of Chemistry, Cambridge, **2001**, pp. 102 – 117.
[2] R. B. Mujumdar, L. A. Ernst, S. R. Mujumdar, C. J. Lewis, A. S. Waggoner, *Bioconjugate Chem.* **1993**, *4*, 105 – 111.
[3] M. Levitus, S. Ranjit, *Q. Rev. Biophys.* **2011**, *44*, 123 – 151.
[4] S. Luo, E. Zhang, Y. Su, T. Cheng, C. Shi, *Biomater.* **2011**, *32*, 7127 – 7138.
[5] K. Licha, U. Resch-Genger in *Comprehensive Biomedical Physics* (Ed.: A. Brahme), Elsevier, Oxford, **2014**, pp. 85 – 109.
[6] A. Mishra, R. K. Behera, P. K. Behera, B. K. Mishra, G. B. Behera, *Chem. Rev.* **2000**, *100*, 1973 – 2012.
[7] a) K. Licha, B. Riefke, V. Ntziachristos, A. Becker, B. Chance, W. Semmler, *Photochem. Photobiol.* **2000**, *72*, 392 – 398; b) L. Strekowski, M. Lipowska, G. Patonay, *Synth. Commun.* **1992**, *22*, 2593 – 2598; c) J. Pauli, K. Licha, J. Berkemeyer, M. Grabolle, M. Spieles, N. Wegner, P. Welker, U. Resch-Genger, *Bioconjugate Chem.* **2013**, *24*, 1174 – 1185; d) J. H. Flanagan, S. H. Khan, S. Menchen, S. A. Soper, R. P. Hammer, *Bioconjugate Chem.* **1997**, *8*, 751 – 756.
[8] a) B. Chipon, G. Clavé, C. Bouteiller, M. Massonneau, P.-Y. Renard, A. Romieu, *Tetrahedron Lett.* **2006**, *47*, 8279 – 8284; b) C.-H. Tung, *Pept. Sci.* **2004**, *76*, 391 – 403.
[9] D. Komljenovic, M. Wiessler, W. Waldeck, V. Ehemann, R. Pipkorn, H.-H. Schrenk, J. Debus, K. Braun, *Theranostics* **2016**, *6*, 131 – 141.
[10] a) G. T. Hermanson, *Bioconjugate Techniques*, 3rd ed., Academic Press, Boston, MA, **2013**, pp. 787 – 838; b) F. M. Veronese, *Adv. Drug Delivery Rev.* **2002**, *54*, 453 – 456.
[11] Y. Lu, S. E. Harding, A. Turner, B. Smith, D. S. Athwal, J. G. Grossmann, K. G. Davis, A. J. Rowe, *J. Pharm. Sci.* **2008**, *97*, 2062 – 2079.
[12] a) A. Abuchowski, J. R. McCoy, N. C. Palczuk, T. van Es, F. F. Davis, *J. Biol. Chem.* **1977**, *252*, 3582 – 3586; b) A. Abuchowski, T. van Es, N. C. Palczuk, F. F. Davis, *J. Biol. Chem.* **1977**, *252*, 3578 – 3581.
[13] S. J. Koussoroplis, G. Paulissen, D. Tyteca, H. Goldansaz, J. Todoroff, C. Barilly, C. Uyttenhove, J. Van Snick, D. Cataldo, R. Vanbever, *J. Controlled Release* **2014**, *187*, 91 – 100.
[14] J. R. McCombs, S. C. Owen, *AAPS J.* **2015**, *17*, 339 – 351.
[15] a) S. K. Bhatia, L. C. Shriver-Lake, K. J. Prior, J. H. Georger, J. M. Calvert, R. Bredehorst, F. S. Ligler, *Anal. Biochem.* **1989**, *178*, 408 – 413; b) L. C. Shriver-Lake, B. Donner, R. Edelstein, B. Kristen, S. K. Bhatia, F. S. Ligler, *Biosens. Bioelectron.* **1997**, *12*, 1101 – 1106; c) V. H. Routh, C. J. Helke, *J. Neurosci. Methods* **1997**, *71*, 163 – 168.
[16] P. Cuatrecasas in *Biochemical Aspects of Reactions on Solid Supports* (Ed.: G. R. Stark), Academic Press, Stanford, CA, **1971**, pp. 79 – 109.
[17] a) V. Wycisk, J. Pauli, P. Welker, A. Justies, U. Resch-Genger, R. Haag, K. Licha, *Bioconjugate Chem.* **2015**, *26*, 773 – 781; b) M. Wyszogrodzka, K. Möws, S. Kamlage, J. Wodzińska, B. Plietker, R. Haag, *Eur. J. Org. Chem.* **2008**, 53 – 63.
[18] V. Wycisk, K. Achazi, P. Hillmann, O. Hirsch, C. Kuehne, J. Dernedde, R. Haag, K. Licha, *ACS Omega* **2016**, *1*, 808 – 817.
[19] O. Mader, K. Reiner, H.-J. Egelhaaf, R. Fischer, R. Brock, *Bioconjugate Chem.* **2004**, *15*, 70 – 78.
[20] R. B. Mujumdar, L. A. Ernst, S. R. Mujumdar, A. S. Waggoner, *Cytometry* **1989**, *10*, 11 – 19.
[21] S. Derer, P. Bauer, S. Lohse, A. H. Scheel, S. Berger, C. Kellner, M. Peipp, T. Valerius, *J. Immunol.* **2012**, *189*, 5230 – 5239.
[22] K. Licha, P. Welker, M. Weinhart, N. Wegner, S. Kern, S. Reichert, I. Gemeinhardt, C. Weissbach, B. Ebert, R. Haag, M. Schirner, *Bioconjugate Chem.* **2011**, *22*, 2453 – 2460.
[23] R. P. Haugland in *Monoclonal Antibody Protocols* (Ed.: W. C. Davis), Humana Press, Totowa, NJ **1995**, pp. 205 – 221.

Received: January 17, 2017
Version of record online April 13, 2017

